DOE/PC/91034--T10

QUARTERLY TECHNICAL PROGRESS REPORT NUMBER 12

THE ECONOMICAL PRODUCTION OF ALCOHOL FUELS FROM COAL-DERIVED SYNTHESIS GAS

CONTRACT NO. DE-AC22-91PC91034

REPORTING PERIOD:

July 1, 1994 to September 30, 1994

SUBMITTED TO:

Document Control Center
U.S. Department of Energy
Pittsburgh Energy Technology Center
P.O. Box 10940, MS 921-118
Pittsburgh, PA 15236-0940

SUBMITTED BY:

West Virginia University Research Corporation
on behalf of West Virginia University
213 Glenlock Hall
Morgantown, WV 26506

October, 1994

TABLE OF CONTENTS

LIST OF TABLES

LIST OF FIGURES

Executive Summary

Both plug-flow microreactor systems at WVU are now functioning. Screening runs on these systems were started using carbide and nitride catalysts first, to avoid any question of contamination of the system with sulfur. The carbide and nitride catalysts are characterized by high activity but low selectivity towards alcohols. The chevrel-phase catalysts tested have much lower activities but may be more selective to alcohols. One reason for the low activity may be the relatively small specific surface area of these materials, as currently synthesized. Catalyst synthesis procedures are attempting to offset this tendency, and also to characterize and prepare sulfide catalyst by other approaches.

At UCC&P, test runs on the reactor system have commenced. Higher alcohols up to butanol were observed and identified at high temperatures.

Modelling studies have concentrated on the catalytic membrane reactor. The partial pressure of the higher-alcohol lump has been shown to decrease monotonically with position in the membrane, with the largest value occuring in the permeate (tube) side of the membrane.

The topical report, originally submitted last quarter, was revised after some errors were found. This report includes the design and economics for the seven cases discussed in previous quarterly reports. In the topical report, it is shown that a judicious choice of coal:natural gas feed ratio to the alcohol synthesis process allows the Shell Gasifier to be nearly competitive with natural gas priced at of $3.00/MMBtu. The advantage of the Shell Gasifier over the Texaco Gasifier is that the former produces a syngas with a lower H_2:CO ratio. When the feed to the process is coal only, there is no difference in the projected economics that would favor one gasifier over the other.

The algorithm for process optimization has been completed. A publication detailing the optimization algorithm has been prepared.

The potential of co-generation of electric power with higher alcohol fuel additives has been investigated. Preliminary results have revealed that a once-through alcohol synthesis process with minimal gas clean-up may provide an attractive alternative to current designs given the prevailing economic status of IGCC units. This status may be further enhanced by considering the value of lower emissions level associated with this power generation technology given the current trend toward more stringent emission standards.

Fuel testing was delayed by problems in obtaining all of the necessary equipment. The equipment has now arrived and the experiments have begun.

TASK 1 REACTION STUDIES

1.1 Introduction

The objective of Task 1 is to prepare and evaluate catalysts and to develop efficient reactor systems for the selective conversion of hydrogen-lean synthesis gas to alcohol fuel extenders and octane enhancers.

Task 1 is subdivided into three separate subtasks: laboratory and equipment setup; catalysis research; and reaction engineering and modeling. Research at West Virginia University (WVU) is focused on molybdenum-based catalysts for higher alcohol synthesis (HAS). Parallel research carried out at Union Carbide Chemicals and Plastics (UCC&P) is focused on transition-metal-oxide catalysts.

1.2 Accomplishments, Results and Discussion

1.2.1 Laboratory Setup

At WVU, we have completed setting up the two reactor systems as plug-flow microreactors. Reactions using the same MeOH synthesis catalyst, from UCC&P, under the same conditions, showed that the results obtained from the two reactors were not distinguishable. This indicates that catalyst screening can be carried out in the two reactors simultaneously. Details have been provided in MS37.

At UCC&P, we have greatly improved our analytical capabilities this quarter, and expect further significant improvements in the next quarter. Most of July was spent developing a GC method using our single-valve sampling system. We purchased packed columns at the advice of ChrompakR, and reduced our sample loop size. We overcame a problem of switching columns between two key components, and we improved our measurement of hydrogen concentrations by altering the method by which the integrator measured hydrogen peaks. We developed a method to determine response factors experimentally for condensable gases, and we are continuing to expand our collection of retention times and response factors for products and side-products of the HAS reactions.

We have recently purchased a Hewlett-Packard ChemStationR for gas chromatograph data handling (UCC&P-funded). Installation is scheduled for October. This purchase will tremendously improve our capabilities to store and manipulate our data.

1.2.2 Molybdenum-Based Catalyst Research

At WVU, we commenced the screening of catalysts in our reactor systems during this quarter. The initial catalysts tested were carbide and nitride species, i.e., not sulfides. This was to avoid any question of reactor contamination. Some sulfide catalysts have also been tested. The catalysts tested were:

1. Potassium-doped molybdenum nitrides (K_xMoN, where x = 0, 0.1, 0.3 and 0.5);
2. Cesium-doped molybdenum nitrides (Cs_xMoN, where x = 0.1, 0.3 and 0.5);
3. Iron carbide (Fe_3C) and iron nitride (Fe_3N);
4. Cobalt/Tungsten mixed-metal carbide (Co_6W_6C);
5. Chevrel-phase sulfides: $Co_{1.6}Mo_6S_8$, $HoMo_6S_6$, $SnMo_6S_8$ and $Ni_{1.6}Mo_6S_8$.

For the screening runs, reaction temperatures were generally programmed from 200°C to 400°C at a rate of 10°C/hour. For some of the carbides and nitrides, and for all of the sulfides, the reactor temperature was also programmed down from 400°C to 200°C at a rate of 10°C/hour after the reactor temperature reached 400°C. The product was analyzed every 2 hours. The pressure was 750 psig. The space velocities were 12,000 or 6,000 l/h/kg-catalyst. The H_2-to-CO feed ratio was 2 in almost all the cases.

Details for the K- and Cs-doped molybdenum nitrides catalysts have been given in MR35 and MR36.The activities for these catalysts are similar. The catalysts have no activity at temperatures below 250°C. Above 250°C, CO conversions increase with an increase in temperature. The doped alkali metals tends to decrease CO conversion. The selectivity pattern for MeOH for these two groups of catalysts are similar. Maxima were observed at around 300°C. The K-doped catalysts showed higher MeOH selectivity than Cs-doped catalysts. Catalysts with high doping levels (0.3 and 0.5) gave higher MeOH selectivity than those with low doping levels (0.1 or 0). Because large amounts of hydrocarbons were formed, identification of higher alcohols is very difficult with these catalysts using the current analysis scheme. High concentrations of C_1-C_3 hydrocarbons (which were identified with confidence) and numerous peaks for $C_{\geq 4}$ hydrocarbons and higher alcohols in the chromatogram suggest that the formation of C_4-C_6 hydrocarbons is high. Correspondingly, the formation of higher alcohols is probably low. Better product analysis techniques are needed. These are currently being pursued.

The results with iron carbide and nitride catalysts have been described in detail in MS35. At 250°C, the CO conversion for Fe_3C is about 90%. A maximum 10% MeOH selectivity was observed for Fe_3C catalyst at the lowest temperature tested, 200°C.

The cobalt/tungsten carbide, Co_6W_6C was obtained commercially. As a catalyst, this material shows about 15% activity and 45% selectivity to MeOH. See Figures 1 and 2.

The activities of Chevrel-phase sulfides are very low (see MS37). At the temperature range of 200-400°C, the maximum CO conversion is less than 0.3% when 0.5 g catalyst is used. However, the selectivity to MeOH is relatively high, about 60-70% at temperatures around 300°C. Formation of higher alcohols is likely but, because of the low conversions, has not been unambiguously confirmed at the present time.

With regard to the synthesis and characterization of the Chevrel phases, the surface area of $Ni_{1.6}Mo_6S_8$ was determined to be 0.17 m^2/g using BET. The low surface area results in extremely low catalytic activity for these materials. Consequently, the synthesis procedure

was modified slightly and six grams of both $Co_{1.63}Mo_6S_8$ and $Ni_{1.6}Mo_6S_8$ have been synthesized and submitted for catalytic evaluation. We are now in a position to make 10 to 12 grams of Chevrel phase materials in one reaction. These will be made as the need arises. A series of the K- and Cs- based Chevrel-phase materials have been synthesized and will be evaluated following the transition metal/lanthanide Chevrel phase compounds.

In the area of synthesis by vapor-phase decomposition, the focus has been to characterize more fully the series of iron carbonitrides prepared from the gas phase reactor (see TPR 11 for synthesis details) and to produce and characterize mixed-metal carbonitrides containing molybdenum and iron. C/N analyses (Dumas combustion method) and surface area analyses (using BET) have been accomplished for the iron nitrides and carbides prepared by reactions between $Fe(CO)_5$ and ammonia at temperatures ranging from 300 to 1000 °C. See Table I and Figures 3a and 3b. For each of the eight experiments, materials were isolated from three different parts of the reaction tube: collection frit (A), exhaust end of reaction tube (B), and the inner surface of the water jacket (C). The "A" and "C" materials were evaluated by X-ray powder diffraction (Figures 4a and 4b, respectively) and elemental analyses (Table I). For the "A" series, a crystallographic change from hexagonal (low temperature) to orthorhombic (high temperature) occurs between 600 and 700 °C (Figure 4a). For materials formed between 300 and 600°C, powder patterns have been indexed to hexagonal $Fe_xN(C)$ $(3>x>1)$, while at temperatures above 700°C, an orthorhombic Fe_3C forms in addition to elemental iron. Generally, for the "A" series, the carbon and nitrogen amounts vary in an indirect manner (Figure 3a), with the maximum nitrogen and carbon percentages achieved at 500 and 700°C, respectively. The carbon and nitrogen amounts are constant from 800 to 1000°C. The surface areas (BET) of iron carbonitrides (series "A") were determined. The surface area trend (see Figure 3b) for the "A" materials correlates with the crystallographic phase transition observed by X-ray powder diffraction. In the "C" series, all the patterns can be indexed to hexagonal Fe_3N, Fe_3C, $Fe_{2.5}N$ and orthorhombic Fe_2N, with the best fit being $Fe_3N(C)$ (see Figure 4b). The highest amount of nitrogen for any of the iron samples was found for 700°C at 12.50%. Carbon and nitrogen amounts generally decrease with temperature for the "C" series. (As noted earlier, materials from the "A" and "C" series can be pyrophoric! "C" materials have been shown to combust during grinding.) The effect of these changes on catalytic performance will be determined.

Mixed metal carbonitrides have been produced from the co-decomposition of $Mo(CO)_6$ and $Fe(CO)_5$ in ammonia at 800 °C. By varying the flow rates of He and ammonia and the temperatures of each carbonyl, we have shown that mixed iron/molybdenum carbonitrides can be produced with varying metal ratios. See Table II for synthetic conditions and crystallographic trends. The metal ratios were determined by EDS, using a ZAF correction. The lattice parameters were determined by Rietveld refinement of the X-ray powder data. Three important observations can be made from the mixed metal experiments. First, the materials II48b and II49C are single phase. Second, the unit cell undergoes an isotropic expansion as more molybdenum is introduced in the reaction (see Figure 5 and Table II). Third, II55C appears to be a disproportionation product of the reaction. The sharper peaks identified in the X-ray powder pattern of II55C match those in I110A (Fe_3N with no

molybdenum) and broad peaks corresponding to an amorphous phase are also present, indicating a multiphase material. It appears that there is a limit to the solid solution of molybdenum in Fe_3N between an atomic Mo/Fe ratio of 1:2.8 and 1:2.1. The effect of these phase changes on catalytic performance will be investigated.

Two compounds, $K_2Mo_3S_{13}$ and $Cs_2Mo_3S_{13}$, have been prepared as precursors to alkali-modified MoS_2. Conventional attempts to prepare MoS_2 have been accomplished by thermally decomposing ammonium paramolybdate in hydrogen sulfide, or thermally decomposing ammonium thiomolybdate in an inert or sulfur-rich environment. To complete the synthesis, the alkali is typically added to the MoS_2 by incipient-wetness techniques. The method of doping and the nature of the alkali precursor play a critical role in the selectivity and the activity of the alkali modified MoS_2. By using $K_2Mo_3S_{13}$ and $Cs_2Mo_3S_{13}$, the alkali can be included in the MoS_2 in a one-step process, thereby eliminating variations due to the alkali addition step and allowing a supported alkali-modified MoS_2 to be prepared, due to the solubility of $K_2Mo_3S_{13}$ and $Cs_2Mo_3S_{13}$ in polar solvents.

1.2.3 Transition-Metal-Oxide Catalyst Research

At UCC&P, we conducted our first HAS run in the microreactor. One gram of 11-DAN-45 catalyst was used. Reactions were carried out under 1:1 synthesis gas for about eight days at a pressure of about 750 psig and at temperatures of 300°C, 350°C, and 400°C, respectively. At 300°C, methanol and hydrocarbons formed, but no butanol was detected. At 350°C, butanol was observed in small quantities. At 400°C, butanol was present in larger quantities.

We also conducted a microreactor run using a standard methanol catalyst (United Catalysts Inc. - C18-7). One gram of catalyst was reduced in size to 40 - 50 mesh and then mixed with like-sized glass beads. 1:1 synthesis gas was reacted over the catalyst for about two weeks under 600- 750 psig and 250-300 °C. GC analysis indicated that the reaction produced mainly methanol with smaller amounts of short-chain alkanes as byproducts under all reaction conditions. CO_2-free selectivity to methanol was lower than expected. There was no obvious indication of catalyst deactivation.

With the departure of Dick Nagaki from the project, we have been practicing the production of catalyst supports this quarter to ensure that these supports are being made with the same consistency and quality as in the past. Surface area measurements and performance studies with previously-tested catalyst formulations have indicated that our catalyst support manufacturing skills are now satisfactory.

1.2.4 Reaction Engineering

In this quarter, we have studied a catalytic membrane reactor (CMR), in which the membrane itself is catalytic or is impregnated with the catalyst. The schematic diagram of a CMR for the production of higher alcohols from synthesis gas is shown in Figure 6. In this

setup, hydrogen and carbon monoxide flow through the shell side of the CMR. They permeate through the membrane and react inside the membrane to form higher alcohols and other products. We adopted the isothermal "Single Cell Model" used by Sun and Khang (1988), in which the contents in the feed chamber (shell side) and the permeate chamber (tube side) are assumed, respectively, to be well-mixed, and no longitudinal variations are considered.

Using the Simplifed Reaction Scheme of Tronconi et al. (1987), we obtained eight ordinary differential equations (ODEs). This set of ODEs is of the two-point boundary-value type with essentially a boundary condition of the third kind at both boundary points. These equations were solved using two independent methods, namely, finite difference method and false transient method, to ensure that the numerical results obtained are correct and accurate. In the finite difference approach, the eight boundary-value type ODEs were converted into a system of nonlinear algebraic equations, which were then solved simultaneously using NEQNF, an IMSL subroutine. In the false transient approach, on the other hand, the boundary-value type ODEs were converted into initial-value type partial differential equations, which were solved by the method of lines. The numerical results obtained from both schemes, with error tolerances of 1.0×10^{-12} for the false transient method and 1.0×10^{-10} for the finite difference method, are plotted in Figures 8-11. In general, the values obtained using these two different schemes are quite close to each other. In both methods, we fixed the H_2-to-CO ratio in the feed at 1.0 and the ratio of total pressure in the feed side to the permeate side as 0.6.

In Figure 7, the dimensionless partial pressures of hydrogen and carbon monoxide inside the membrane are plotted as a function of dimensionless radius. The hydrogen and carbon monoxide diffuse continuously through the membrane and react inside the membrane to form the oxygenated species. The partial pressures of both hydrogen and carbon monoxide can be seen to decrease in a linear fashion with the log of dimensionless radius from the feed (shell) to the permeate (tube) side.

Figure 8 shows the variations of partial pressures of methanol and methane inside the membrane. The partial pressures of both species are found to be maximum in the region close to the permeate side ($\xi_m = 0.4$ for CH_4 and $\xi_m = 0.2$ for CH_3OH). In Figure 9, the variation of the partial pressure of water inside the membrane is plotted; the maximum is found to occur at around $\xi_m = 0.25$. The partial pressure of the higher-alcohol lump, HA, varies monotonically inside the membrane as shown in Figure 10, with the maximum occurring in the permeate (tube) side.

In Figure 11, the conversions of carbon monoxide in a PMR and a CMR are compared in a semi-log plot. Here the CO conversion is defined as

$$X = 1 - \{(x_{co} + y_{co})/(x_{co}^{\circ} + y_{co}^{\circ})\} \qquad (6)$$

and the mean residence time is taken as the volume of catalyst divided by the volumetric

flow rate passing through the catalyst. It can be seen that the conversion of carbon monoxide in a PMR is much higher than that in a CMR. This can be attributed to the effect of transmembrane total pressure drop on the equilibrium conversion of methanol synthesis reaction. There is a decrease in the number of moles when carbon monoxide reacts with hydrogen to form methanol. Sun and Khang (1990) have shown that a CMR does not increase the yields of equilibrium reactions in which the number of moles decreases. Hence the amount of methanol formed in a CMR is much less than that in a packed-bed membrane reactor (PMR). This consequently leads to a decrease in the number of moles of HA formed. In Figure 12, the mole fraction of HA in a CMR is compared to the mole fraction of HA in a PMR. It can be seen from the figure that the mole fraction of HA in a CMR is considerably less than that in a PMR.

1.3 Conclusions and Recommendations

The plug-flow microreactor system at WVU has been used to screen a number of carbides, nitrides and sulfides as potential HAS catalysts. Typically, the first two types of materials give rise to high conversions of CO but negligible selectivity towards higher alcohols, while the sulfides have low conversions but possibly high selectivity to alcohols. The low conversions are probably due to the low specific surface area of these catalysts, as currently synthesized.

The reactor system at UCC&P is functioning well and will be ready to accept copper-based catalysts for screening, following the plan developed earlier.

We are now in a position to make relatively large amounts (10g) of chevrel-phase materials in one batch. The problem of increasing the specific surface area of the chevrel-phase sulfide catalysts has not yet been solved. Characterizations of the iron carbonitrides and the mixed-metal carbonitrides show interesting compositional and phase changes which may be related to catalytic performance.

The catalytic membrane reactor modelled in this quarter leads to mole fractions of higher alcohols which are much lower than those from the packed-bed membrane reactor. Hence the catalytic membrane reactor should not be used for HAS.

1.4 Future Plans

At WVU, we expect to improve our technique to analyze the product streams so as to obtain unambiguous detection of higher alcohols. The improved technique includes changing columns and procedures as necessary. Further, we expect to repeat the Chevrel-phase runs using larger amounts of catalyst so as to avoid the problems inherent with low conversions from the reactor. The Co_6W_6C catalyst appears promising, and will be doped with alkali metals to test for higher-alcohol selectivity.

The next phase of Chevrel-phase synthesis will involve two approaches to higher-surface-

area Chevrel compounds. The first approach will use water-soluble precursors to prepare supported materials, while the second approach will investigate using the gas-phase reactor for bulk Chevrel-phase production. Further, based on the vapor-phase mixed-metal carbonitride work, mixed-metal sulfides containing iron and molybdenum or cobalt and molybdenum will be made.

At UCC&P, we anticipate having copper-based catalysts to test in the second half of October. We expect to use the scheme of attack described in TPR11.

References

1. Sun, Y. and S.J. Khang, Ind. Eng. Chem. Res., **27**, 1136 (1988).
2. Sun, Y.and S.J. Khang, Ind. Eng. Chem. Res., **29**, 232, (1990).
3. Tronconi, E., N. Ferlazzo, P. Forzatti and I. Pasquon, Ind. Eng. Chem. Res. **26**, 2122 (1987)

Table I. Experimental Parameters and Analytical Results for Materials Formed by the Thermal Decomposition of $Fe(CO)_5$ in Ammonia Vapor at 300 to 1000 °C.

Reference #	I116	I115	I114	I113	I112	I110	I117	I118
Temperature (°C)	300	400	500	600	700	800	900	1000
Carbon, %, "A" ("C")[1]	1.47	2.14	2.08	6.25	6.39 (3.3)	3.99	4.19 (2.2)	3.55 (2.5)
Nitrogen, %, "A" ("C")[1]	6.91	10.23	11.36	3.53	1.85 (12.5)	0.35	0.05 (9.0)	0.05 (7.7)
C + N, %, "A" ("C")[1]	8.38	12.37	13.44	9.78	8.24 (15.8)	4.34	4.24 (11.2)	3.60 (10.2)
Surface Area, m^2/g, "A"[1]	9.45	11.93	12.88	13.67	6.69	7.59	N/A	2.05

[1] "A" corresponds to iron products isolated in a ceramic collection frit;
"C" refers to materials isolated in the water jacket region of the tube (inlet end of reactor).

Table II. Experimental conditions for the thermolysis of $Fe(CO)_5$ and $Fe(CO)_5/Mo(CO)_6$ in ammonia at 800°C.

Reference # (metals present)	Variac[1] Setting	$Fe(CO)_5$ Temperature	Gas Flow Rates (ml/min)[2]			Lattice Parameters	
			NH_3	He (Mo)	He (Fe)	a (Å)	c (Å)
I110C (Fe)	12	Ambient	170	0	100	4.751	4.3986
II48B ($Mo_1Fe_{3.1}$)	12	Ambient	170	100	100	4.8169	4.4791
II49C ($Mo_1Fe_{2.8}$)	14	0°C	170	100	100	4.8702	4.5385
II55C ($Mo_1Fe_{2.1}$)	16	0 °C	170	100	100	4.75	4.4

[1] The tube containing the $Mo(CO)_6$ was wrapped with a four-foot heating tape connected to a 140V variac. The number indicates the percentage of 140 volts applied to the heating tape.

[2] Ammonia and He (Mo) are passed over the heated $Mo(CO)_6$, while He (Fe) is passed through the tube containing the liquid $Fe(CO)_5$.

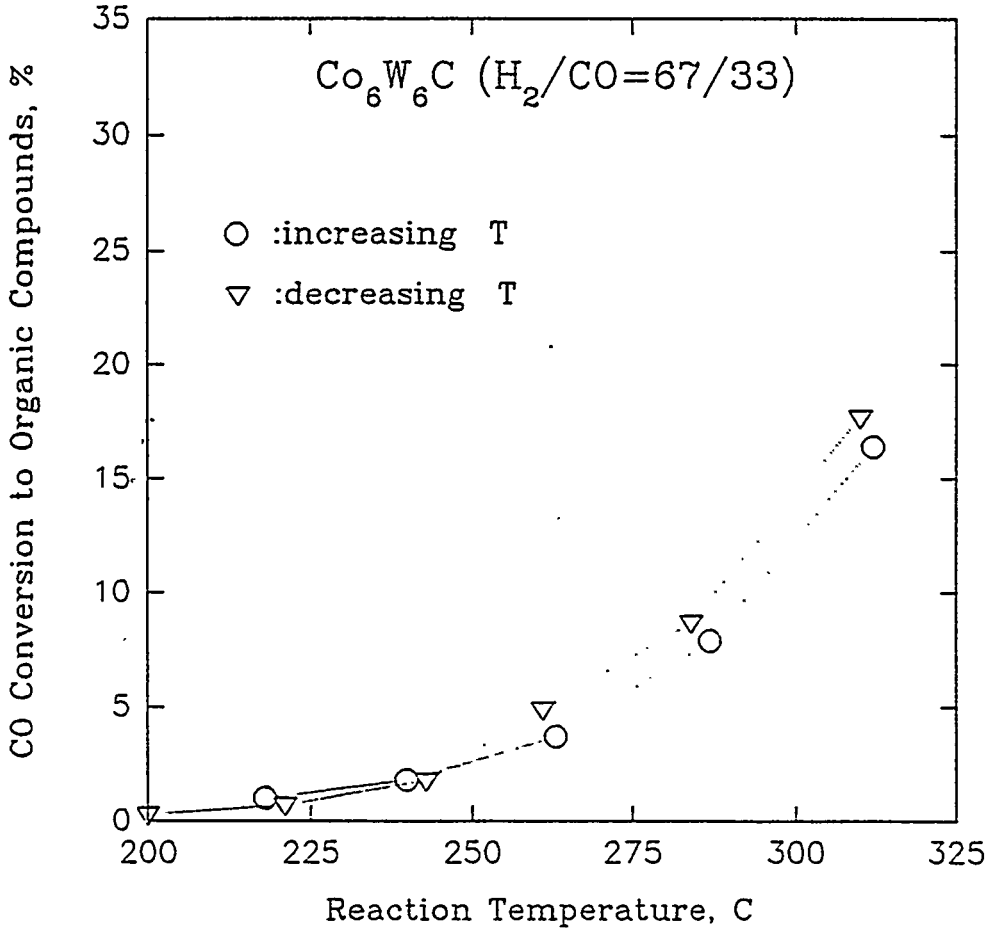

Figure 1. Conversion of cobalt–tungsten carbide catalyst as functions of temperature and history.

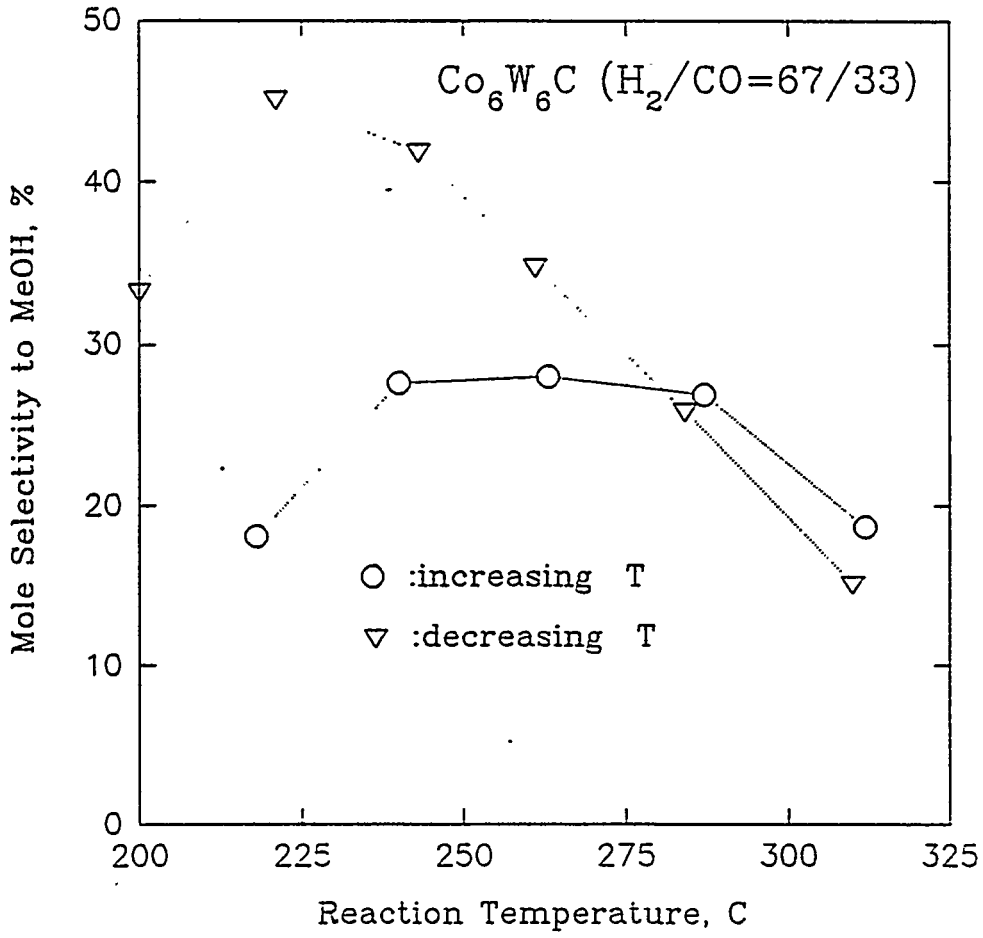

Figure 2. Selectivity of cobalt–tungsten carbide catalyst to alcohols as a function of temperature and history

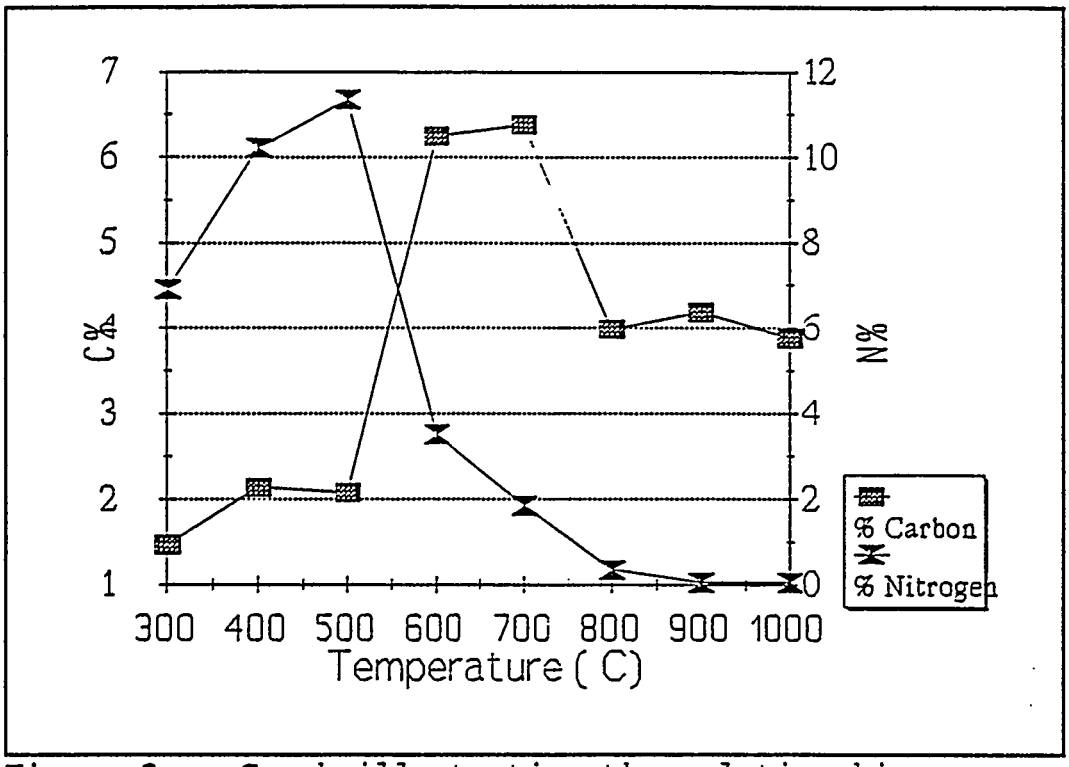

Figure 3a. Graph illustrating the relationship between C or N percentage and reaction temperature for series "A" iron carbonitrides.

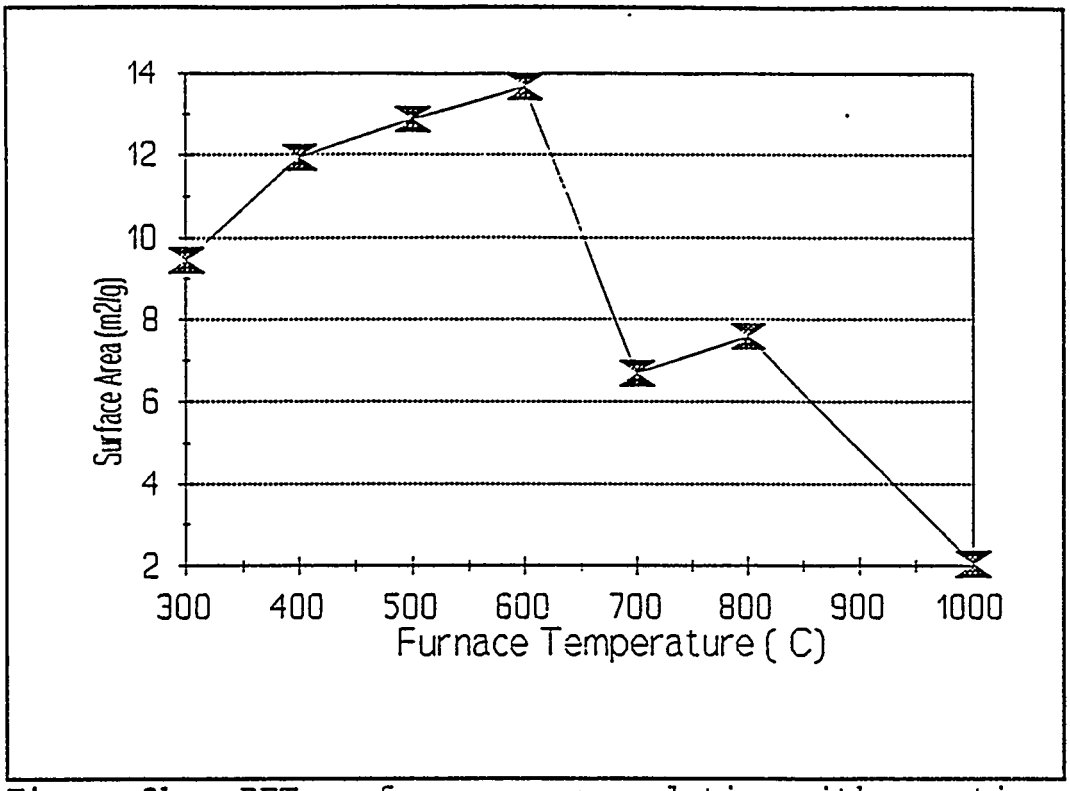

Figure 3b. BET surface area correlation with reaction temperature for "A" iron carbonitrides prepared by the gas phase decomposition of $Fe(CO)_5$ in a helium/ammonia gas stream.

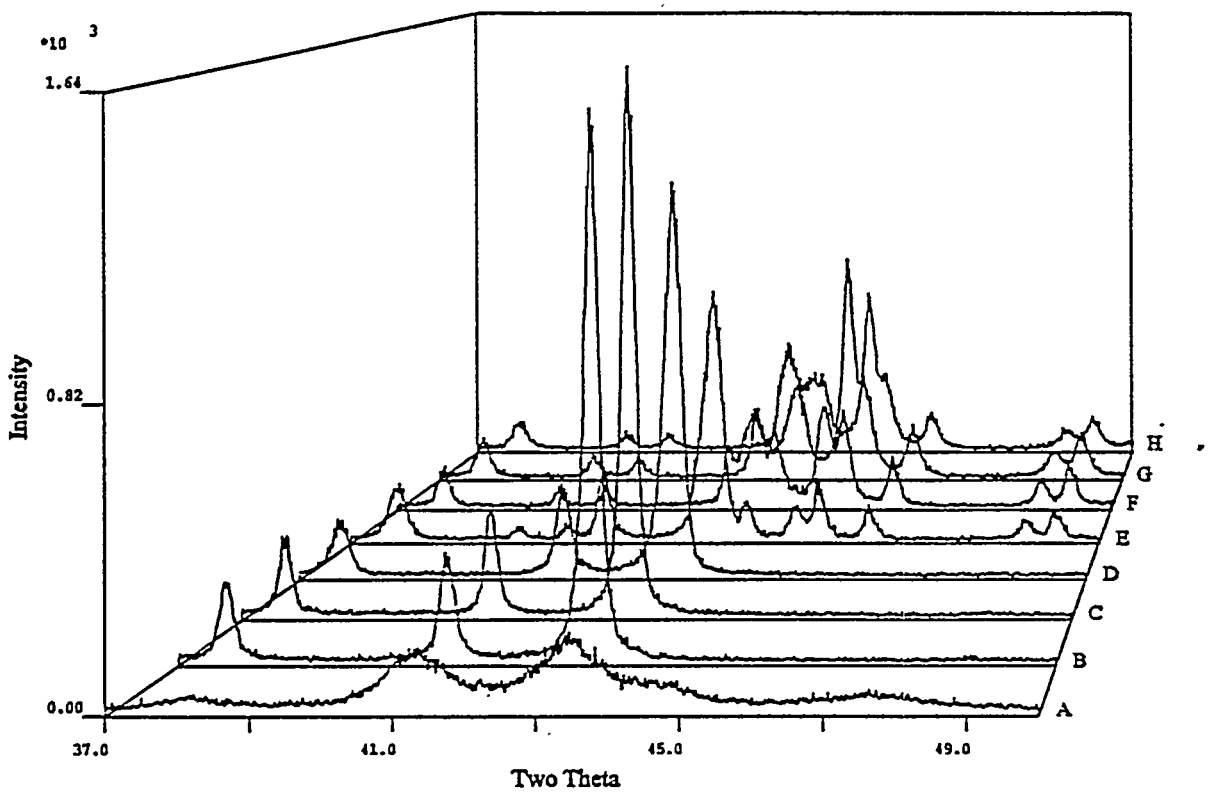

Figure 4A X-ray diffraction patterns for iron carbonitrides (A series) produced from the thermolytic decomposition of $Fe(CO)_5$ with ammonia vapor at (A) 300 , (B) 400, (C) 500, (D) 600, (E) 700, (F) 800, (G) 900 and (H) 1000 °C.

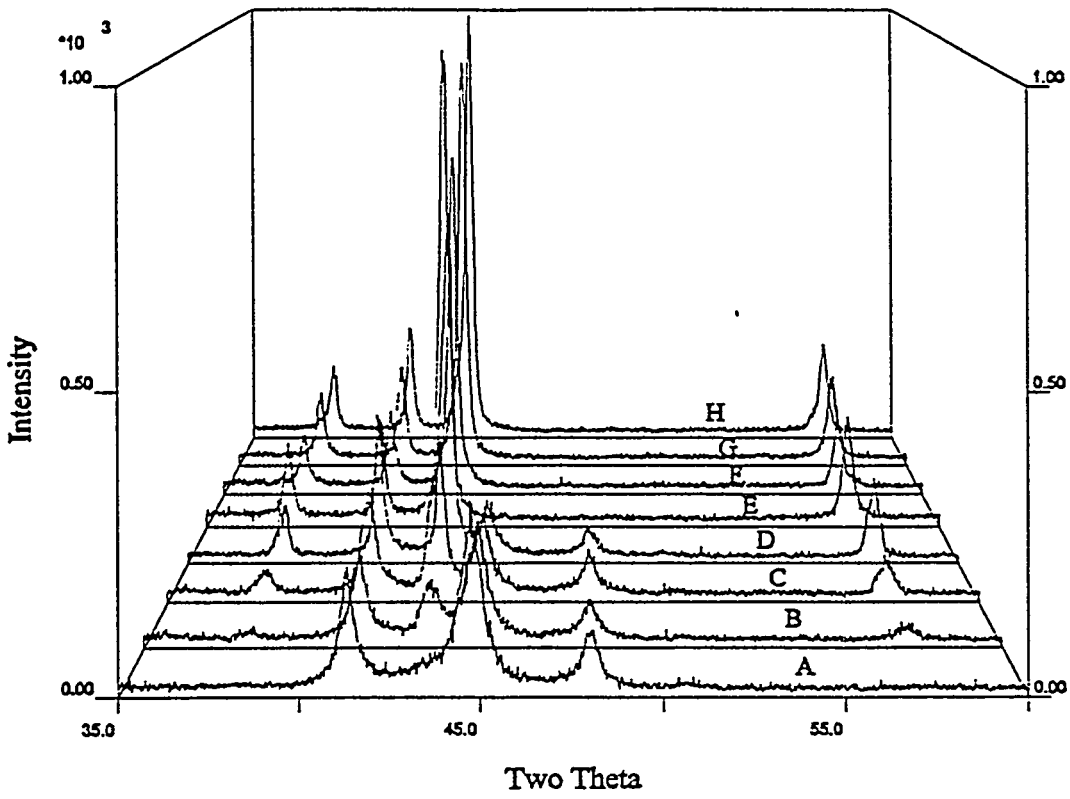

Figure 4b. X-ray diffraction patterns for iron carbonitrides (C series) produced from the thermolytic decomposition of $Fe(CO)_5$ with ammonia vapor at (A) 300 , (B) 400, (C) 500, (D) 600, (E) 700, (F) 800, (G) 900 and (H) 1000 °C.

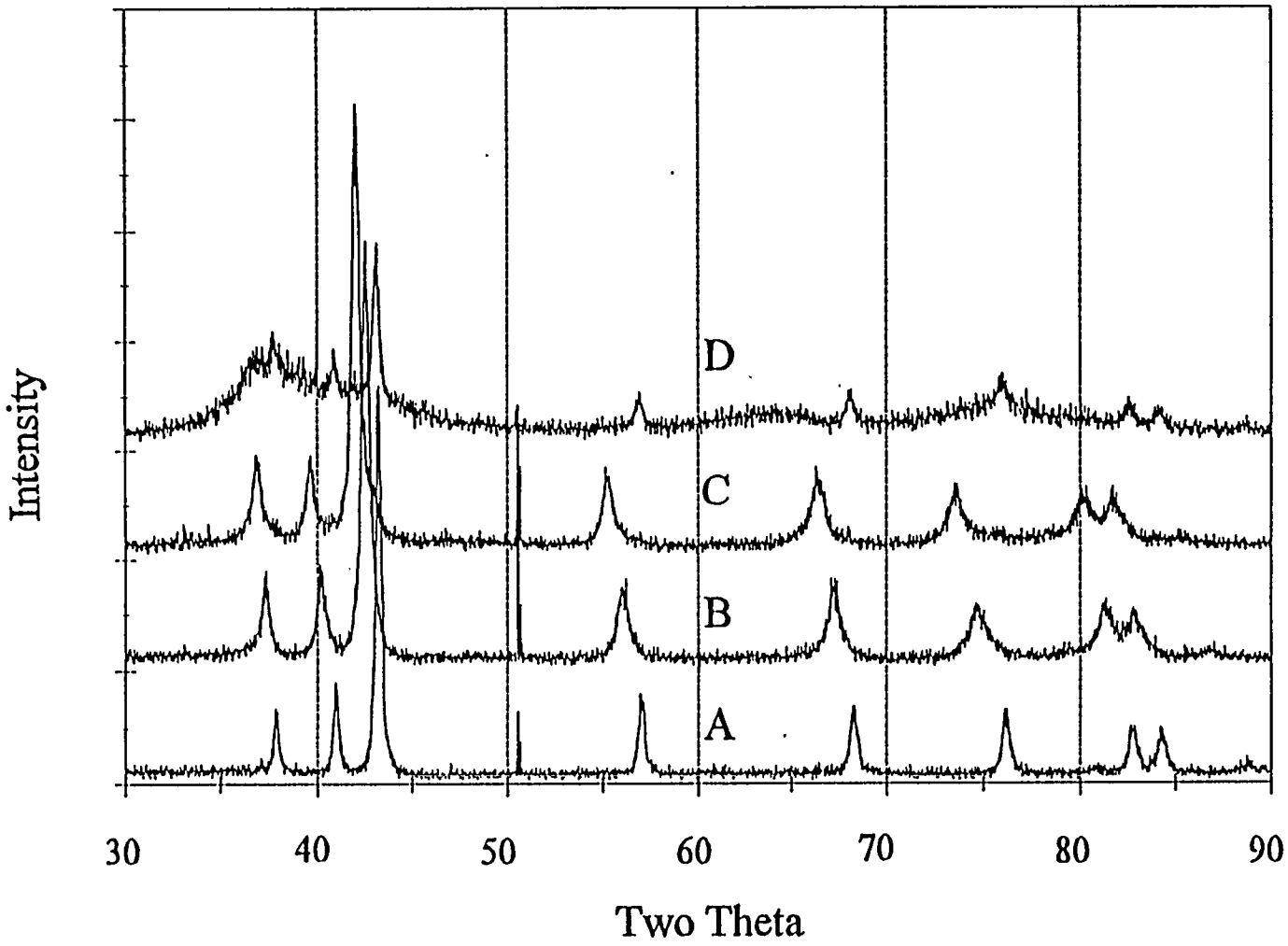

Figure 5. X-ray diffraction plots of materials produced from vapor phase thermal decompositions of iron and molybdenum carbonyls at 800 °C under flowing ammonia. Fe:Mo ratios of products: A) 1:0; B) 3.1:1; C) 2.8:1; D) 2.1:1. Decreasing two theta peak positions reflect the isotropic unit cell expansion with increasing Mo for A-C. The crystalline phase for D is identical to A, but the broad peaks in D result from other less crystalline phase(s).

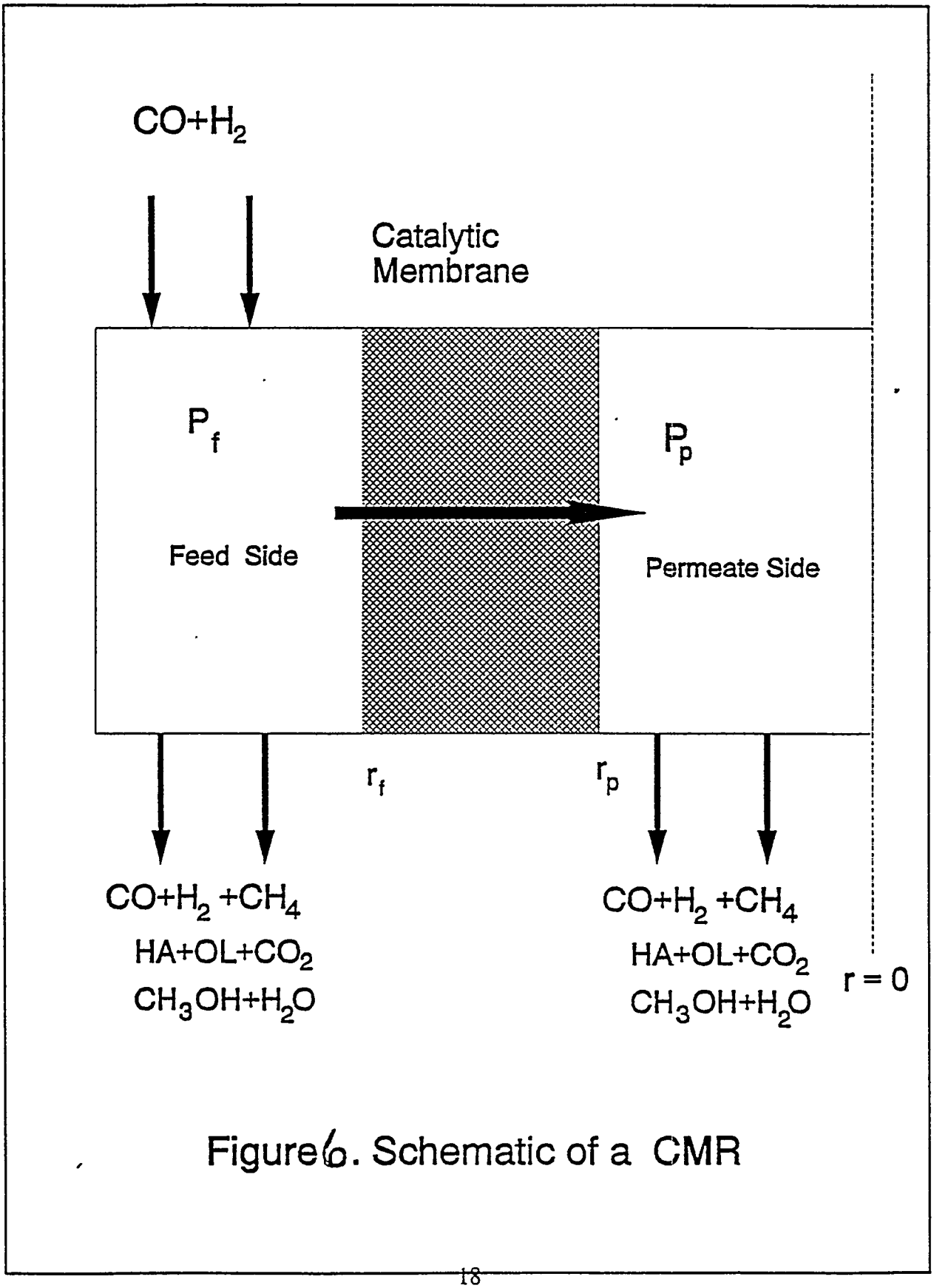

Figure 6. Schematic of a CMR

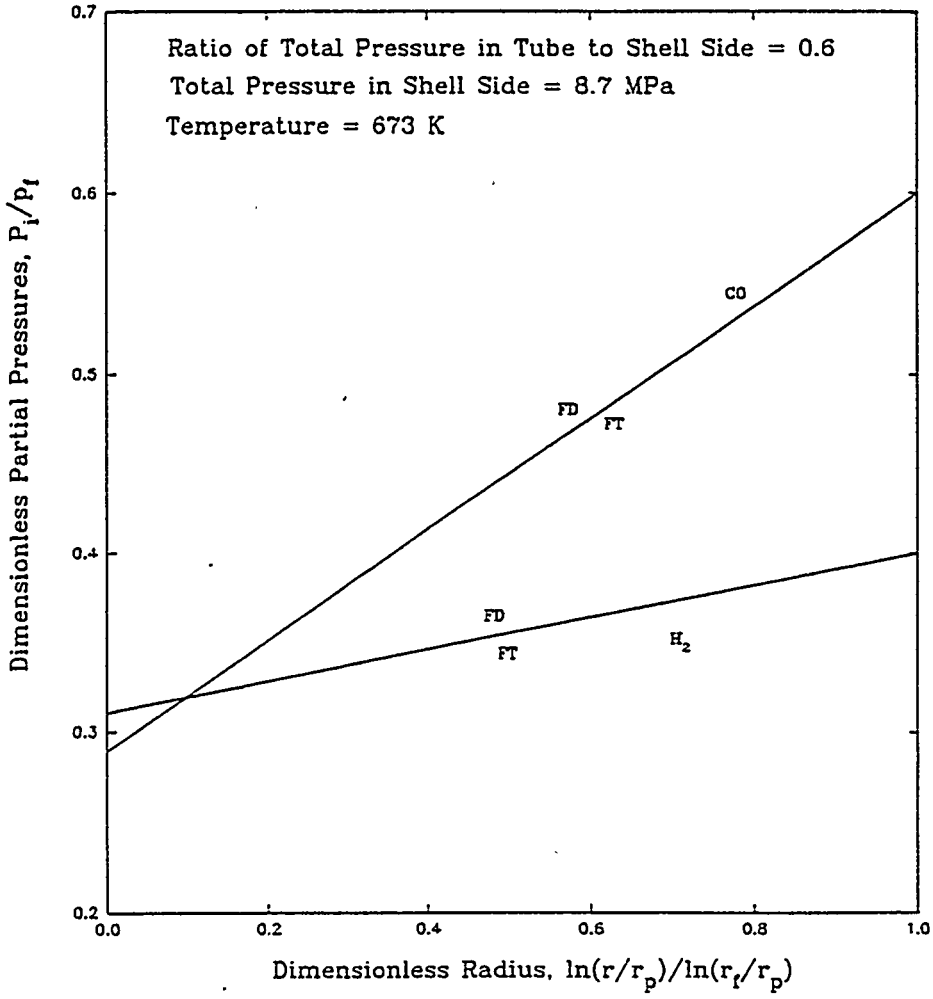

Figure 7. Partial Pressure Profiles of Hydrogen and Carbon Monoxide Inside the Catalytic Membrane of a CMR (FD=Finite Difference Method, FT=False Transient Method)

sep94-7.sp5

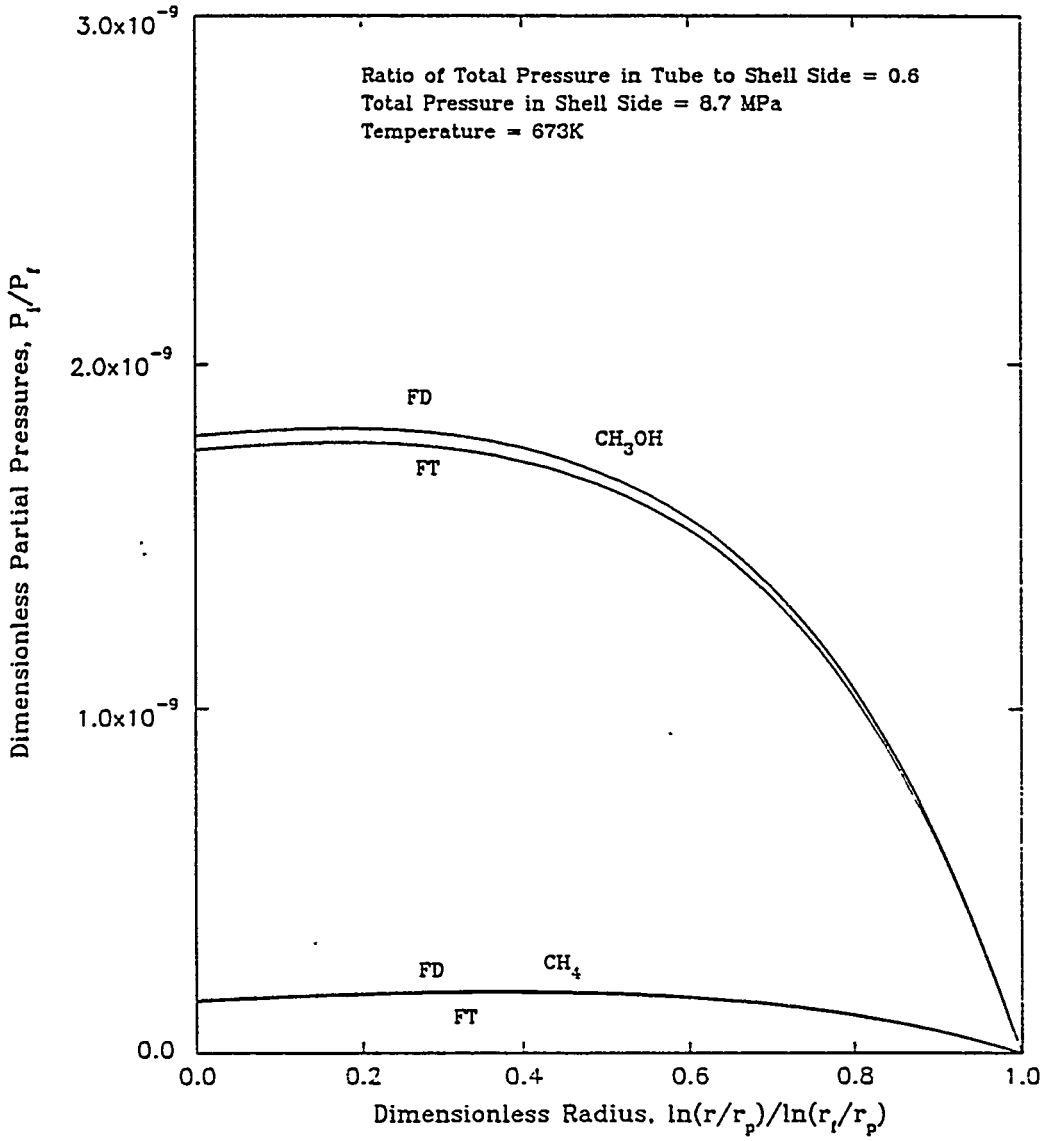

Figure 8. Partial Pressure Profiles of Methanol and Methane Inside the Catalytic Membrane of a CMR (FD = Finite Difference Method, FT = False Transient Method)

sep94-8.sp5

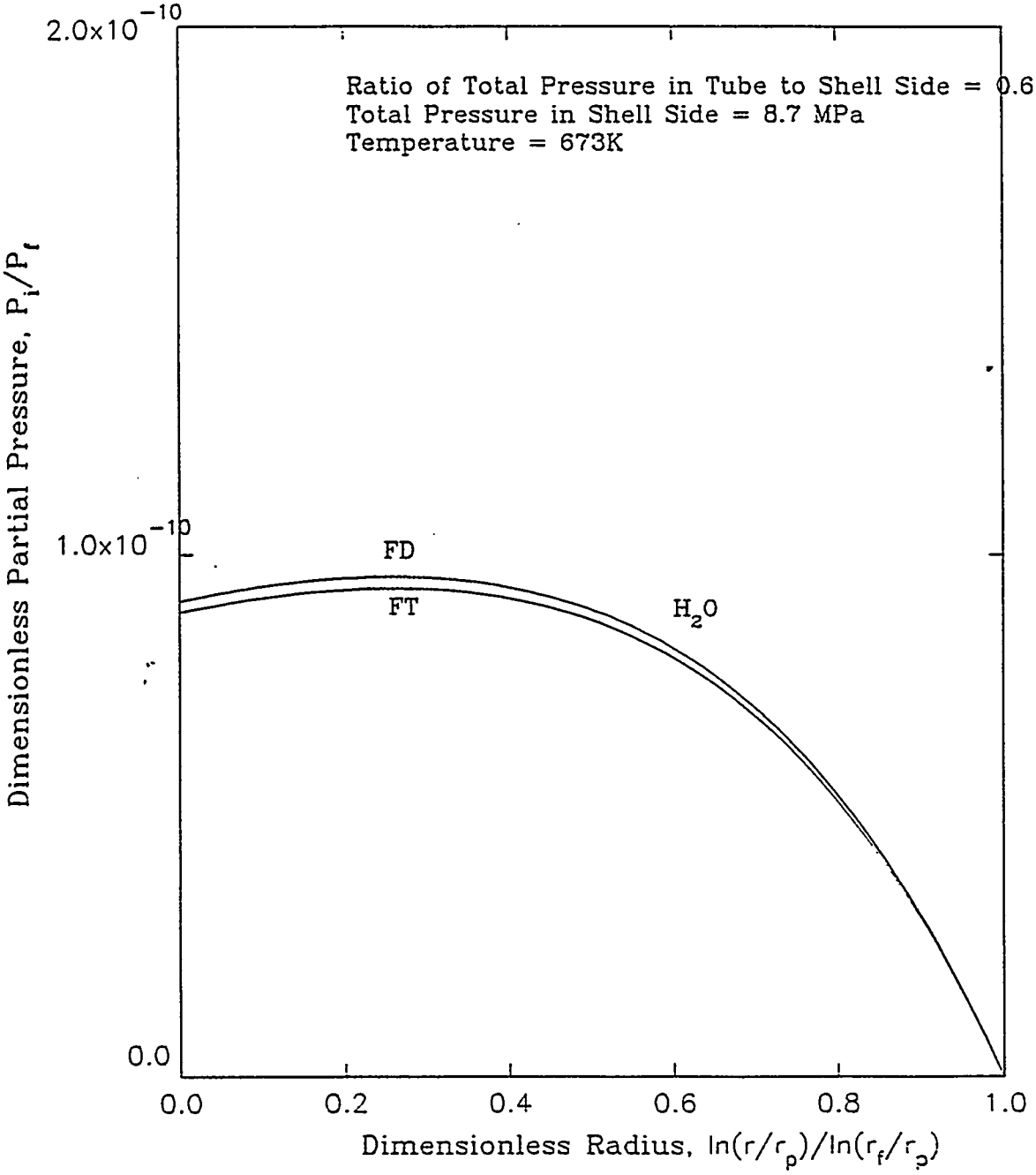

Figure 9. Partial Pressure Profile of Water Inside the talytic Membrane of a CMR (FD = Finite fference Method, FT = False Transient Method)

sep94-9.sp5

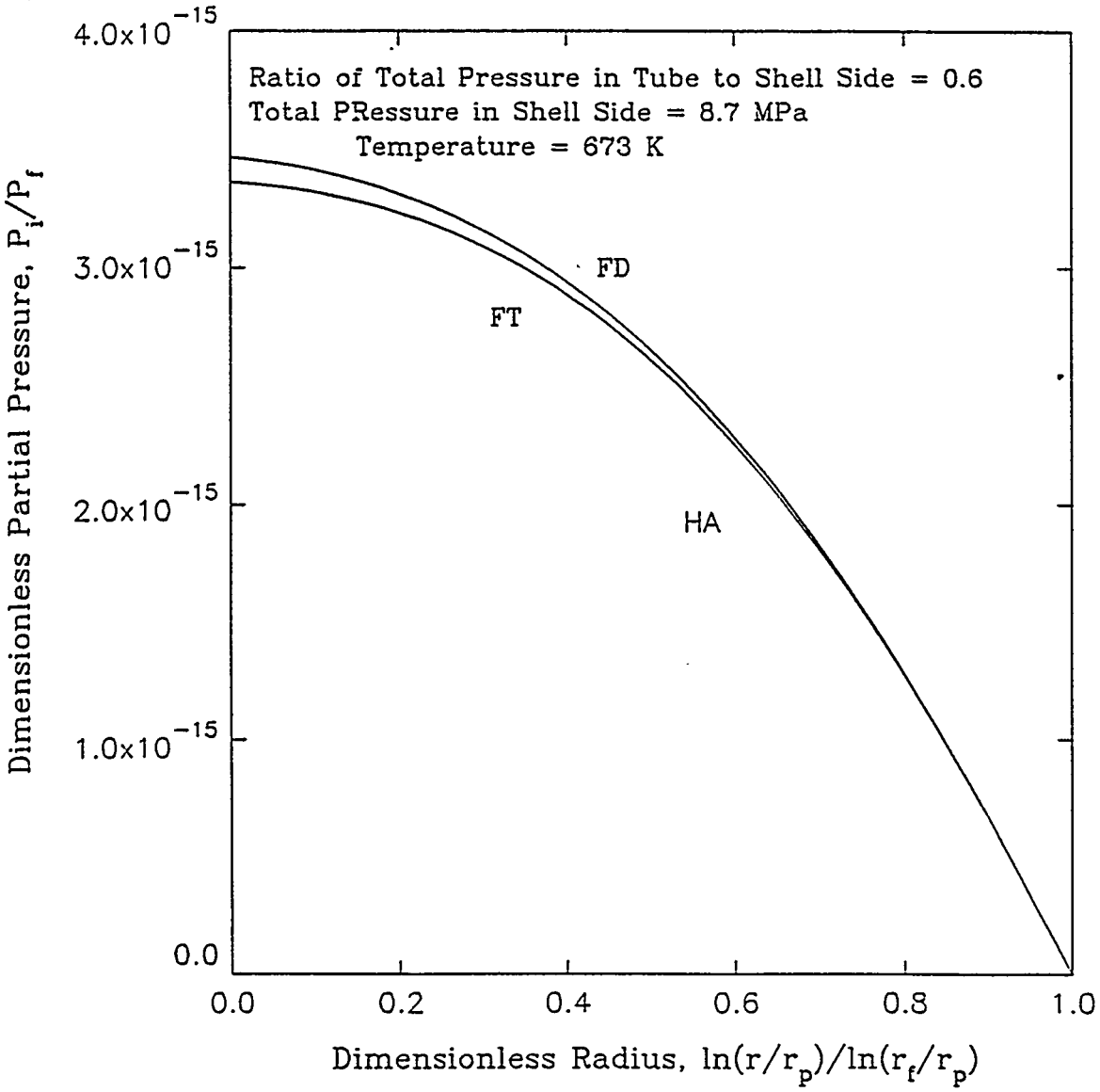

Figure 10. Partial Pressure Profile of Higher Alcohols inside the Catalytic Membrane of a CMR
(FD = Finite Difference Method, FT = False Transient Method)

sep94-10.sp5

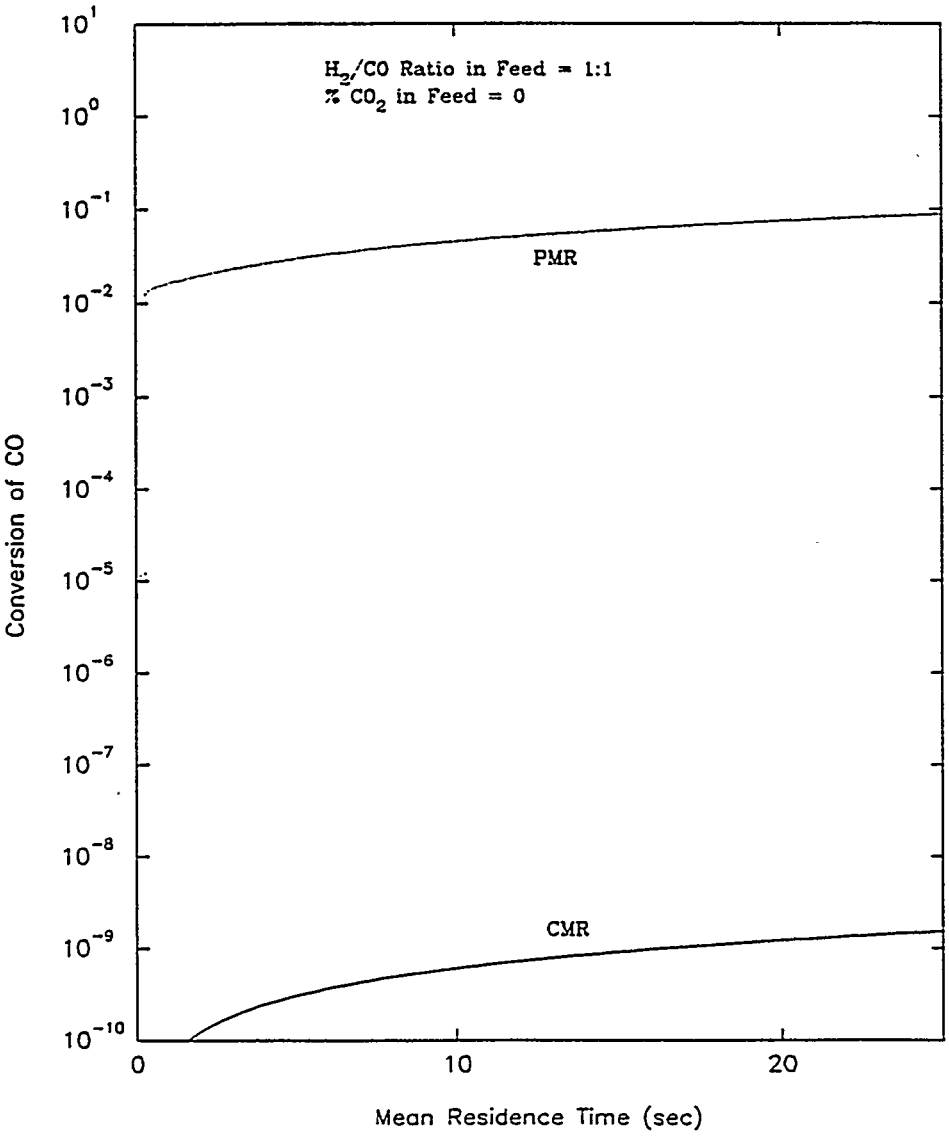

Figure 11. Comparison of Conversion of Carbon Monoxide in a Packed-Bed Membrane Reactor and a Catalytic Membrane Reactor

sep94-11.sp5

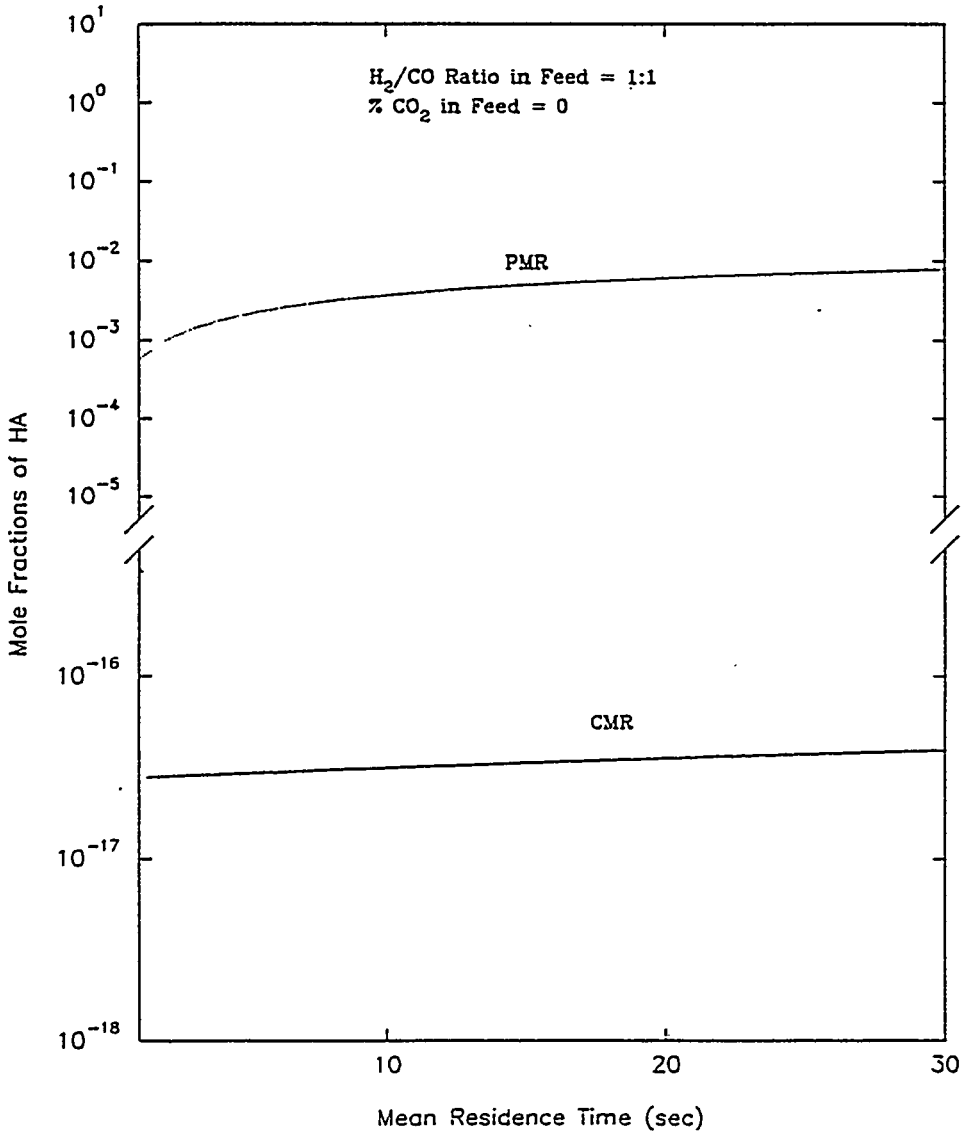

Figure 12. Comparison of Concentrations of Higher Alcohols in a Packed-Bed Membrane Reactor and a Catalytic Membrane Reactor r

sep94-12.sp5

TASK 2. PROCESS SYNTHESIS AND EVALUATION

2.1 Introduction

The topical report, originally submitted last quarter, was revised after some errors were found. This report includes the design and economics for the seven cases discussed in previous quarterly reports.

The algorithm for process optimization has been completed. Hence, work in this area has reached a plateau until more catalyst data are available. A publication detailing the optimization algorithm has been prepared.

The potential of co-generation of electric power with higher alcohol fuel additives is being investigated at this time. Preliminary results of this investigation have revealed that a once-through alcohol synthesis process with minimal gas clean-up may provide an attractive alternative to current designs given the prevailing economic status of IGCC units. This status may be further enhanced by considering the value of lower emissions level associated with this power generation technology given the current trend toward more stringent emission standards.

Research on Monte Carlo sensitivity analysis of the seven design cases has been continuing. All of the effort in the past quarter has been focused on determining reasonable probability distributions for economic and process parameters.

Fuel testing was delayed by problems in obtaining all of the necessary equipment. The equipment has now arrived and the experiments have begun.

2.2 Accomplishments, Results and Discussion

2.2.1 Optimization

During this quarter, we have written an article for publication describing our simulated annealing procedure and results. The optimum design and operation of the alcohol synthesis, separation, and blending part of the process have been studied under various conditions. Our technique includes an enhanced cooling schedule, random move generation (including bi-level moves), and stopping criteria. A copy of this paper is available and will be supplied to PETC after final clearances.

A new graduate student has been started on this project, and he is enhancing the documentation of the FORTRAN program in preparation for the next round of optimization studies.

2.2.2 Economic Analysis

2.2.2.1 Topical Report

Much of the effort this quarter has been focused on completion of the topical report on Case Studies, Design, and Economics. This document includes the process and economic analyses of the seven cases. Overall, it shows that a judicious choice of coal:natural gas feed ratio to the alcohol synthesis process allows the Shell Gasifier to be nearly competitive with natural gas priced at 3.00/MMBtu. The advantage of the Shell Gasifier over the Texaco Gasifier is that the former produces a syngas with a lower H_2:CO ratio. When the feed to the process is coal only, there is no difference in the projected economics that would favor one of these gasifiers over the other. In the

latter case, the H_2:CO ratio is adjusted by water-gas shift.

Details of the analysis can be found in the topical report.

2.2.2.2 Economics of Power Generation

A review of the literature on the economics of IGCC power generation units has been completed. The results of this investigation suggest that IGCC facilities are currently competitive with existing coal plants upgraded to meet Federal emissions standards. On average the current installed capital cost of these units is approximately the same as conventional coal units employing modern emissions reduction technologies. However, if the environmental costs and benefits of the two technologies are factored into the analysis, IGCC units may ultimately prove to be more economical than conventional facilities given the trend of more stringent emissions standards. The primary advantage may be directly attributed to the overall efficiencies of the two processes. The higher efficiency of IGCC units enables them to generate more electricity for a given quantity of fuel, thereby reducing emissions.

Efficiency in power generation is linked to environmental benefits in two ways. First, benefits can be directly related to declines in energy input requirements per unit of output, which ultimately translate into a reduction in the quantity of pollution generated per unit of electricity produced. The levels of reduction, however, are dependent upon the pollutants under consideration. Pollutants such as CO_2 and SO_2, for example, are fuel dependent. Therefore, emissions of these pollutants will be in direct proportion to the type and quantity of fuel used in the generation process. However, other pollutants such as NO_x, CO, and VOC's are technology dependent and the quantity of these pollutants emitted during the generation process depends more on the technology used rather than the amount and type of fuel used.

Second, improvements in energy efficiency may also generate ancillary benefits by reducing the environmental impacts caused by factors other than the combustion of fossil fuels at power generation facilities. The end use of energy at these facilities accounts for only a portion of the overall environmental impact for any given fossil fuel. Therefore, decreasing the fuel requirements for a given level of power production not only reduces the level of pollutants at the generation facility, it also reduces environmental degradation related to the production and processing of fossil fuels by reducing the need to carry out these activities. Efficiency can, therefore, have a strong cumulative effect on reducing environmental impacts associated with the use of fossil fuels as a result of this two-fold effect.

Other advantages of IGCC units may be directly attributed to the inherent flexibility of these systems. Their modular design lends itself readily to phased implementation and provides for easy expansion to meet changes in regional power demands. Additional flexibility is also provided by the combined cycle portion of the plant which can be fueled by virtually any combustible material. Slip streams of syngas may also be taken during off peak periods and used to produce by-products such as higher alcohols thus enabling the facility to run at full capacity during these periods. However, the additional cost of the alcohol synthesis block must be factored into the cost of electricity for these facilities before any definitive conclusion may be drawn with regard to the economic feasibility of such a process.

2.2.3 Monte Carlo Simulation of Process Uncertainties

We have completed the initial probability distributions for our input economic parameters and for some of our process parameters. Work is continuing on the formulation of the appropriate probability distributions for the catalyst performance characteristics. Additional information from Union Carbide and Chemicals Corporation has been received for this task.

The preliminary scoping simulations scheduled for this quarter have been rescheduled for the coming quarter.

2.2.4 Fuel Testing

Activities for the previous quarter on the CFR project can be summarized in three areas: hardware, fuels, and testing.

2.2.4.1 Hardware

Following a long delay at the mass flow controller supplier, the bag sampling system has been completed. This system consists of lines to capture diluted exhaust both in teldar sampling bags, deionized water, as well as silica cartridges. In trial testing conducted during September, this system has worked well. A schematic of this system is shown in Figure 2.1.

2.2.4.2 Fuels

All fuels that are needed to make the blends are now on site. Additionally, all equipment needed to blend them is also here. The fuel blends to be tested are described in the previous quarterly report.

2.2.4.3 Testing

Trial testing for the engine and the gas sampling systems has been underway during September. Baseline conditions for the engine will be those used for the motoring fuel test described in ASTM 05.04. Highlights of this test include a compression ratio of 6.86:1, spark timing of 19 degrees before top dead center, and an engine speed of 900 RPM. For fuels testing, the engine will be run at the same compression ratio and speed, with the spark timing set at MBT, MBT minus five degrees, MBT plus five degrees. Equivalence ratio will be adjusted for 0.9, stoichiometric, and 1.1. Variations in spark timing and equivalence ratio will give a total of nine tests for each fuel.

Analysis of the exhaust samples has shown that the dilution ratio used to take the samples were not high enough. The dilution ratio has been increased, and testing now depends on scheduling time with the gas analyzers.

2.3 Conclusions and Recommendations

Confronted with more stringent emission standards, electricity producers will inevitably begin to rely more heavily on less polluting, more efficient technologies like IGCC. The ability of these facilities to produce higher alcohols during peak demand periods may provide the transportation sector with valuable fuel oxygenates while reducing the cost of peaking power. However, the marginal cost of producing the higher alcohols in this manner needs to be determined and needs to be compared to the marginal benefits associated with the production of these higher alcohols.

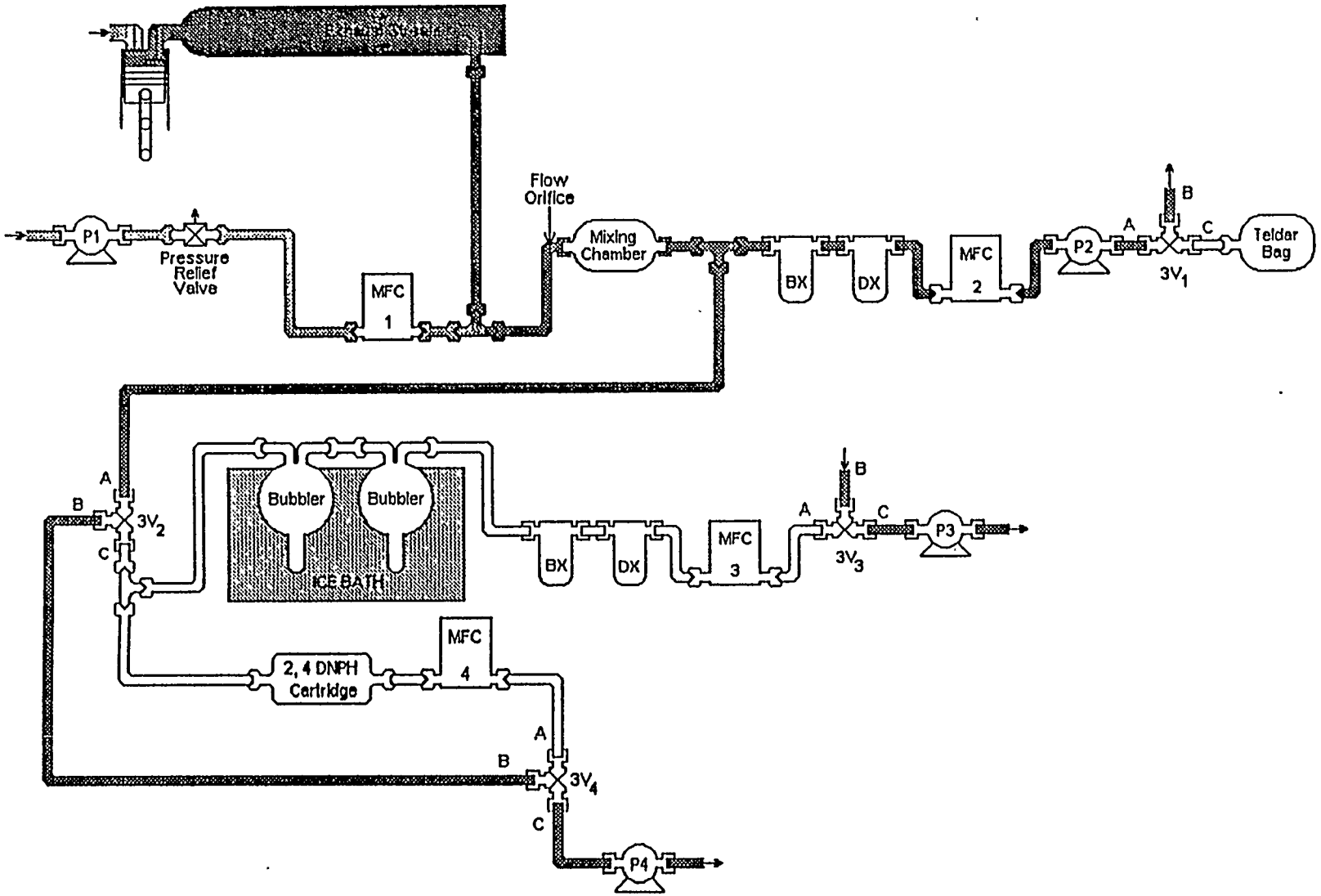

Figure 2.1: Schematic of the Bag Sampling System

Given the economics of IGCC power generation and the potential to produce higher alcohols at the facilities during peak periods, it may be worth while to consider modifying the most favorable base case to produce electricity as the primary product and higher alcohols as by-products. This should require only a few minor modifications.